



STATE UNIVERSITY OF NEW YORK  
AT STONY BROOK

COLLEGE OF  
ENGINEERING

Report No. 45

DISLOCATION DYNAMICS  
IN PURE IRON BY COMBINATION  
FORWARD-REVERSE STRAIN RELAXATION

by

R. Rosenberg

May, 1965

*Spec*  
*TA1*  
*.N532*  
*No. 45*  
*C. 2*

Dislocation Dynamics in Pure Iron by  
Combination Forward-Reverse Strain Relaxation

by

R. Rosenberg

State University of New York at Stony Brook

and

Brookhaven National Laboratory, Upton, New York

## ABSTRACT

Specimens of Ferrovac "E", decarburized iron, irradiated Ferrovac "E", and 700 ppm C-iron were strained 10 percent, held in the loaded condition for specified times and then unloaded to zero applied stress. Resulting reverse relaxation curves were not logarithmic but followed the general form,  $\dot{\gamma}_R = At_R^{(m-1)}$ . Two stages of reverse relaxation were noted for Ferrovac "E", stage I  $< 1$  min. and stage II  $> 2$  min. Both provided negative values for  $m$ , and reflected tangling of dislocations and pinning by accumulation of carbon during reverse flow for stages I and II, respectively. Decarburization caused an increased tangling rate and conversion of stage II to logarithmic behavior ( $m=0$ ). Irradiation reduced cross glide and tangling, and removed carbon from the lattice, probably as carbon-defect pairs. Excess carbon had little effect, except to make  $m$  more negative during stage II. Pinning of dislocations in tangled networks by dislocation redistribution and carbon atmosphere took place during the forward relaxation cycle. Unpinning of these dislocations during reverse flow resulted in a positive  $m$  in stage I. Yield point analysis substantiated the pinning and unpinning results. Observation of the magnitude of  $A$  and the change with holding time showed forward relaxation in Ferrovac "E" and 700 ppm C-iron to be parabolic ( $m_h > 0$ ), the configurations produced in the irradiated samples to have a lower degree of tangling and more "free" dislocation segments, and the configuration in the decarburized samples to be heavily tangled.

## INTRODUCTION

The fundamentals of gross dislocation flow and deformation in pure iron might best be determined by considering dislocation interactions, slip systems, and slip configurations rather than activation mechanisms for movement of individual segments. Much useful work has been done using the interrupted forward creep method, most extensively by Conrad<sup>(1)</sup>, and has resulted in information concerning activation volumes and energies for dislocation motion over ranges of temperature and stress. The results, however, appear to be independent of gross dislocation behavior, interactions and possible changes in slip mechanism with change in test condition, which seem to govern the deformation characteristics. The techniques of electron and optical microscopy have been used to illustrate dislocation and slip line configurations produced under various test conditions, as shown by Keh and Weissmann<sup>(2)</sup> for example, but do not consider the kinetics of their formation.

A method currently being used to study dislocation kinetics is the evaluation of the exponent  $n$  in the relation  $\bar{v} = (\tau^*/\tau_0)^n$ , first proposed by Gilman and Johnston<sup>(3)</sup>, where  $\tau^*$  is the effective stress aiding dislocation movement and  $\bar{v}$  is the average dislocation velocity. Stein and Low<sup>(4)</sup> have measured  $n$  in Fe-3Si by the etch pit technique which essentially involves the movement of "free" dislocations and is not meant to be applicable to effects of changes in configuration and resulting interactions, although they were able to predict the yield point dependence on temperature by assuming a critical velocity. Michalak<sup>(5)</sup> has shown the relationship between  $n$  and the forward creep

method in pure iron and has measured the dependence of dislocation velocity on stress and temperature. To do this, the values of  $n$  obtained at different strain levels were extrapolated back to zero strain to obtain  $n^*$ , which then was used to obtain the velocity dependence. For comparison of test results it is necessary to work in a range of strain and temperature where the configuration and slip systems operative are unchanging, which could be restrictive. Noble and Hull<sup>(6)</sup> have shown  $n$  to be related to change in configuration by using a stress-relaxation technique, but the interpretation was clouded by the non-separability of the participating processes.

Reverse relaxation, or the torsional after-effect, is a time dependent plastic recovery subsequent to loading and holding cycles. The recovery is affected by (a) an internal localization of dislocations into high stress regions, or (b) a surface barrier in which either dislocation emigration is prevented<sup>(7)</sup> or a difference in elastic constants exists between metal and oxide<sup>(8)</sup>. In either case, release of the applied stress will cause a strain reversal by an unbalanced stress field. In the present work the reverse relaxation technique was used to investigate changes in forward dislocation configuration with time, separation of processes contributing to forward and reverse dislocation motion, and to show the effects of structural changes, such as irradiation damage, on each of the processes separately. For this work, all specimens were chemically polished immediately prior to testing to minimize the surface effect and to allow study of the internal properties. The driving force for reverse relaxation (internal stress field), and the number of

mobile dislocations present at the time of load removal are controlled by the forward strain and relaxation cycles; thus changes in configuration during forward flow can be detected by measuring changes in the reverse rate. Also, the characteristics of the reverse relaxation curves provide information concerning the relative ease of movement of the dislocations through the lattice. An advantage of using reverse movement rather than forward movement to study lattice effects is the absence during reverse flow of such contributors to forward creep as recovery and cell formation, significant multiplication of new dislocation segments by double cross glide and changes in gross configuration.

The reverse relaxation,  $\gamma_R$ , is generally considered to be logarithmic and the data presented as in Eq.(1).

$$(1) \quad \gamma_R = \beta + \alpha \ln t_R$$

Roberts and Brown<sup>(9)</sup> derived this relationship for relaxation in zinc single crystals by assuming the dimensional representation of Eq.(2) to be applicable, in which  $N_{mR}$  is the number of contributing disloca-

$$(2) \quad \dot{\gamma}_R = b A_0 N_{mR} \bar{V}_R$$

tion segments,  $\bar{V}_R$  is their average velocity equal to  $v \exp\{-(u_0 - v\tau^*)/kT\}$ ,  $\tau^*$  is the effective stress at any time and "v" the activation volume. The stress,  $\tau^*$ , was written as  $\tau^* = \tau'_i - \tau_A - \theta \gamma_R$ ,  $\tau'_i$  being the internal stress field at  $t_R = 0$ ,  $\tau_A$  the applied stress, and  $\theta$  a work-softening coefficient equal to  $\partial \tau_A / \partial \gamma_R$  at  $t_R = 0$ . By assuming  $N_{mR}$  constant

they arrived at a form of Eq. (1), where  $\alpha = \frac{kT}{v\theta}$  and  $\beta$  contained the constant terms in the form,

$$\beta = \frac{kT}{v\theta} \ln \left[ \frac{\nu b A_0 N_{mR}}{\alpha} \exp \left\{ -\frac{(U_0 - v\tau_i + v\tau_A)\beta}{kT} \right\} \right].$$

The assumption of constant  $N_{mR}$  during relaxation appears questionable in materials where multiple glide and interactions predominate, such as with pure iron in the present work. A preliminary reverse relaxation test did indeed show a significant deviation from logarithmic behavior, prompting a re-evaluation of the variables. One approach would be to vary  $N_{mR}$  with time in the manner suggested by Gilman and Johnston<sup>(3)</sup> in LiF crystals, Eq. (3), and later used by

$$(3) \quad \frac{\partial N_{mR}}{\partial t_R} = K_1 N_{mR} - K_2 N_{mR}^2$$

Li<sup>(10)</sup> to analyze creep rate in metals. The rate constants  $K_1$  and  $K_2$  are for multiplication by double cross glide and removal by tangling, respectively. The resulting expression for the number of dislocations is given in Eq. (4), where  $N_{mi}$  is the initial number of

$$(4) \quad N_{mR} = N_{mS} \left[ 1 - \left( \frac{N_{mi} - N_{mS}}{N_{mi}} \right) e^{-K_1 t_R} \right]^{-1}$$

mobile dislocations and  $N_{mS}$  is the final number ( $t_R \rightarrow \infty$ ) and equal to  $K_1/K_2$ . Assuming, as does Li<sup>(10)</sup>, that the velocity is constant,

$N_{mi} = \dot{\gamma}_{Ri}/b\bar{v}_R$  and  $N_{mS} = \dot{\gamma}_{RS}/b\bar{v}_R$ . If  $K_1$  is small and  $\dot{\gamma}_{Ri} \gg \dot{\gamma}_{RS}$ , which is reasonable for reverse flow, Eq. (4) reduces to the logarithmic form,  $\dot{\gamma}_R = \dot{\gamma}_{RS} + C t_R^{-1}$ . Thus, logarithmic behavior can result from a changing dislocation density at constant velocity, or changing velocity at a constant density. Inserting a combination of both

effects into Eq. (2) leads to the complex form of Eq. (5), where B is equal to  $\frac{v_0}{kT} b A_0 \nu N_{ms} \exp\{-(U_0 - v\tau')/kT\}$  at  $\tau_A = 0$ , and  $A'$  is

$$(5) \quad \delta_R = \frac{kT}{v_0} \ln B \left[ t_R + \frac{1}{K_1} \log \left( \frac{1 - A' e^{-K_1 t_R}}{1 - A'} \right) \right]$$

equal to  $(N_{mi} - N_{mS})/N_{mi}$ . Taking  $K_1$  small reduces the logarithmic term in the bracket to  $\log [1 + A'' K_1 t_R]$ , where  $A'' = A'/(1 - A')$ . This then becomes approximately  $A'' K_1 t_R$  and Eq. (5) reduces to the logarithmic form of Eq. (1) with  $N_{mi}$  replacing  $N_{mR}$  in the constant term,  $B$ . Again, it is not clear that a combination of Eqs. (2) and (3) will lead to a general expression from which deviations from logarithmic behavior can be quantitatively studied. A different, and as yet unknown, relationship for  $\dot{N}_{mR}$  appears to be necessary in place of Eq. (3). Since the number of processes contributing to change in dislocation density during relaxation in pure iron can be formidable and can vary with test conditions, and since the current state of knowledge cannot describe each of the contributors sufficiently, it is doubtful that a workable equation can be found to meet all of the requirements of the present work. It is hoped that the results of this study will lead to such an equation.

It seems advisable for the present to follow Grussard's suggestion<sup>(11)</sup> that, where possible, a general equation of the form,

$$(6) \quad \delta_R = A t_R^{(m-1)}$$



should be used to analyze creep behavior. Changes in characteristics of dislocation movement produce a change in the parameter  $m$ , which thus can be used as a representation of the deviation from logarithmic behavior; that is,  $m = 0$  corresponds to logarithmic creep,  $m > 0$  is a positive, or parabolic deviation, and  $m < 0$  is a negative, or hyperbolic, deviation. Assuming the reverse relaxation data can be plotted in this manner, at least qualitative information concerning the relative ease of dislocation movement can be obtained.

## EXPERIMENTAL PROCEDURE

The materials used in this investigation were Ferrovac "E", 700ppm C-iron, and decarburized Ferrovac "E". A chemical analysis of the Ferrovac is given in Table I.

Table I

	<u>C</u>	<u>O</u>	<u>N</u>	<u>H</u>	<u>Minimum Fe</u>
Ferrovac "E"	30ppm	55ppm	5ppm	.7ppm	99.94

The high carbon material was made by remelting the Ferrovac in vacuum and adding the necessary amount of graphite. The decarburization treatment used was the method of Stein, et al. (12) which consisted of heating samples to 850°C for 72 hours in a dry purified hydrogen atmosphere. Control samples containing C<sup>14</sup> were used allowing a measure of the carbon content after the decarburization treatment. A reasonable estimate based on the counting technique was about 10<sup>-3</sup> ppm. The absence of an upper yield point was further evidence that the carbon was removed in the material used in the present work.

The specimens were swaged to 0.050" D, straightened, cut into two inch lengths, and annealed in vacuum for six hours at 700°C, resulting in an average grain size of 0.040 mm. The decarburized samples had an average grain size of 0.200 mm. Standard Ferrovac "E" samples of the same grain size were prepared by heating in vacuum for 72 hours at 875°C. Samples of Ferrovac "E" were irradiated to 2 x 10<sup>18</sup> nvt (E > 1.45 mev) after the 700°C anneal. All specimens were chemically polished in 70H<sub>3</sub>PO<sub>4</sub> - 30H<sub>2</sub>O<sub>2</sub> immediately prior to testing.

The apparatus used for performing the forward and reverse relaxation studies was essentially the same as that used by Barrett<sup>(7)</sup>, with mechanical modifications for uniform load and unload cycles, and provision for testing at low temperature for future continuation studies. Briefly, a specimen is twisted to a prescribed angle, held under load for a given holding time, and then released. The stress during the twist cycle is measured by using a cantilever beam with an attached SR-4 strain gage as the means of keeping a frictionless top stop from being rotated by the specimen. The force on the beam, or the torque on the specimen, is then plotted on a strain gage recorder, resulting in stress-time curves. Upon load removal, an immediate elastic response takes place followed by a time-dependent untwisting, or reverse relaxation. By using a lamp-mirror-scale arrangement, a surface strain sensitivity of about  $0.6 \times 10^{-6}$  (0.25 mm scale reading) was achieved. The twist rate was  $6 \text{ deg. sec.}^{-1}$  ( $0.157 \text{ min}^{-1}$  surface strain rate), and the angle of twist was 230 deg. (0.10 surface strain).

## EXPERIMENTAL RESULTS

### Ferrovac "E"

A family of reverse relaxation curves for Ferrovac "E" iron, obtained for different holding times after a 0.10 forward strain, is shown in Fig. 1. The abscissa used was  $\log t_R$  to illustrate deviations from logarithmic behavior. The "initial" relaxation rate increased with increasing holding time,  $t_h$ , for at least 20 minutes, and the curves uniformly show a negative deviation. For  $t_h \geq 40$  min., the curves initially deviate positively then transform to a negative deviation at longer relaxation times. Also, the "initial" rate decreases with increasing holding times beyond 40 min.

Replotting the data as  $\log \dot{\gamma}_R = \log A + (m-1) \log t_R$  as suggested by Eq. (6) results in the series of curves in Fig. 2. Consider first the curves for holding times of 5, 10 and 20 minutes (0 and 1 min. curves were not included to avoid unnecessary confusion since they were similar to the 5, 10, and 20 minutes results). The data can be separated into two linear regions, stage I  $< 1$  min. and stage II  $> 2$  min. The curves appear to be approximately parallel in both stages, thus enabling the separation of the forward and reverse processes; that is, the reverse flow mechanisms are independent of holding time, but the absolute magnitude of the constant A is controlled by the forward processes occurring during the holding period. The slopes of the lines in the two stages provide values of  $m < 0$ , the second stage being more negative than the first. The negative  $m$  was implied in Fig. 1, but contribution by more than one mechanism was not obvious. The magnitude of A increased with holding time. The data for  $t_h = 40$  min. shows an initial stage (stage I<sup>1</sup>) where  $m > 0$  and then a final stage

which becomes parallel to stage II of the shorter holding time curves. At  $t_h = 60$  min.,  $m$  is still positive in the initial stage, but lower than that of the  $t_h = 40$  min. curve. Again the final stage is parallel to stage II. After a 120 min. hold apparently all three stages (I, I<sup>1</sup>, II) are present. The value of  $A$  is seen to decrease significantly at the longer holding time.

To summarize briefly, the data has shown the following:

- (1) at least three mechanisms contributing to reverse relaxation have been found, two resulting in negative  $m$  (stages I and II) and one in positive  $m$  (Stage I<sup>1</sup>),
- (2) the negative and positive values of  $m$  are independent and dependent on holding time, respectively,
- (3) the value of  $A$  increases then decreases with holding time, the decrease coinciding with the onset of positive  $m$ .

The following series of tests were run to assist in the identification of the various mechanisms involved, and to show simultaneously the effects of structural changes on the mechanisms.

#### Decarburized iron

Samples of Ferrovac "E" were treated in the manner described in a previous section to reduce the carbon content. Reverse relaxation tests were run over a series of holding times, and the data plotted to provide Fig. 3. The curves again show two stages, the first being similar to stage I in Ferrovac "E", but the second being logarithmic ( $m=0$ ) indicating that removal of stage II results from carbon depletion. Thus, it seems at least one stage, stage II, can be identified as the interaction of moving dislocations with the dissolved carbon in the lattice, most likely by accumulation of an atmosphere, decrease in

velocity, and subsequent pinning. Also, the positive  $m$  stage was not found and  $A$  appeared to be independent of holding time. Since the decarburization treatment produced an increase in grain size, a series of standard Ferrovac "E" samples with the larger grain size was run to determine whether  $m$  depended on the loss of carbon or on grain size. As shown in later summary figures, the values of  $m$  were the same as those found in the smaller grain size samples discussed previously, but  $A$  showed a tendency to be somewhat lower at comparable holding times.

#### Iron - 700ppm carbon

The curves of Fig. 4 represent the results of a series of tests run in samples with an excessive carbon content. The three stages of reverse relaxation previously observed in Ferrovac "E" again are present, but the positive deviation ( $m > 0$ ) appears only after a prolonged holding time of  $10^3$  min., and stage II begins after a longer relaxation period.

#### Irradiated Ferrovac "E"

Test samples of Ferrovac "E" irradiated at  $2 \times 10^{18}$  nvt provided the reverse relaxation curves of Fig. 5. Within limits of error, stage I appears to be logarithmic over all holding times indicating the absence of one of the contributors to negative deviation. Stage II initially shows a large negative deviation ( $m$  more negative than in unirradiated "E"), but quickly becomes logarithmic after  $t_h > 1$  min. The value of  $A$  is not strongly affected by holding time but, as shown in a later figure, first increases then decreases after one minute. To assure that the observations were produced by the irradiation,

irradiated samples were annealed for 2 hours at 400°C, a treatment known to cause reversion of mechanical properties to those of the un-irradiated state. Testing produced results identical to the data of Fig. 2 with one exception, a larger negative deviation was observed in stage II. This could very well be the superposition of the effects of the annealed structure (loops, etc.) on the carbon pinning.

### Summary curves

A comparison of the above findings are illustrated in Figs. 6 and 7 for values of  $m$  and  $A$ , respectively. The significant observations are as follows:

- (1) Stage I - The values of  $m$  for Ferrovac "E", decarburized iron, and 700ppm C-iron all fall within the band  $-.2 > m > -.36$  (for  $t_h < 20$  min.), with the decarburized samples providing the lowest values. At  $t_h = 40$  min., Ferrovac "E" (both grain sizes) shows a positive deviation (stage I<sup>1</sup>,  $m \approx +.4$ ). The 700ppm C-iron shows a gradual decrease in negative  $m$  and becomes positive after a long holding time. No change in  $m$  with holding time is noted in the decarburized samples. The irradiated samples show logarithmic behavior ( $m = 0$ ).
- (2) Stage II - A greater spread in results is noted for the values of  $m$  in this region. Generally  $|m_{\text{E}}| < |m_{700\text{ppmC}}| < |m_{\text{IRR, Ann}}|$ , and  $m_{\text{DECARB}} = 0$ , showing the sensitivity of this test to defects in the structure. A trend seems apparent in Ferrovac "E" and 700ppm C-iron whereby  $m$  decreases at holding times of the same order as those required for the positive deviation of stage I in Ferrovac "E". This would indicate that the phenomenon that gives rise to positive  $m$  also decreases the effectiveness of stage II. A positive  $m$  does not appear

in the 700ppm C-iron at this time, but is found only after much longer holding times.

(3) A values - Ferrovac "E" shows the largest holding time dependence, A first increasing then decreasing at the holding time corresponding to the onset of positive m in stage I<sup>1</sup>. Irradiated "E" and decarburized iron are both comparatively insensitive to holding time, but the absolute magnitudes of A in the irradiated samples are highest of all systems tested. The 700ppm C-iron samples show a less time-dependent A than Ferrovac "E" although both deviate positively from the logarithmic relation  $A = clnt_h$ . The absolute magnitude of A is initially higher in the high carbon material.



## DISCUSSION

Before analyzing the data, an attempt should be made to illustrate the significance of the parameters  $m$  and  $A$  with respect to dislocation motion. Differentiation of Eq. (2) results in,

$$(7) \quad \frac{\partial \dot{\gamma}_R}{\partial t_R} = b A_0 \left[ \bar{V}_R \dot{N}_m + N_m \dot{\bar{V}}_R \right]$$

allowing both the number of mobile dislocations and their average velocity to change. The velocity is dependent on the effective stress driving the dislocations, and assuming the relation  $\bar{V}_R = (\tau_R^* / \tau_0)^n$  to be applicable and  $\tau_R^*$  can be written as  $\tau^* = b A_0 G N_T^{1/2}$ , where the quantity  $N_T$  is the total number of dislocations contributing to the internal stress field in the regions of high stress concentration, the change in velocity can be expressed as,  $\dot{\bar{V}}_R = \bar{V}_R n \dot{N}_T / 2 N_T$ . If the rate of change in the number of dislocation segments contributing to reverse relaxation,  $\dot{N}_m$ , is equal to the negative rate of change of dislocations contributing to the driving stress,  $-\dot{N}_T$ , then Eq.(7) can be written as,

$$(8) \quad \frac{\partial \dot{\gamma}_R}{\partial t_R} = b A_0 \bar{V}_R \left[ 1 - \frac{n N_m}{2 N_T} \right] \dot{N}_m$$

A comparable relationship can be obtained by differentiating Eq.(6), resulting in  $\frac{\partial \dot{\gamma}_R}{\partial t_R} = (m-1) \dot{\gamma}_R t_R^{-1}$ . Inserting  $A_0 b N_m \bar{V}_R$  for  $\dot{\gamma}_R$  and substituting into Eq.(8) gives,

$$(9) \quad m = 1 + t_R \left[ N_m^{-1} - \frac{n}{2} N_T^{-1} \right] \dot{N}_m$$

In pure iron at 10% strain  $N_T \gg N_m$  and the second term can be considered negligible. An approximation of Eq.(9) can then be written,

$$(10) \quad m = 1 + \frac{t_R}{N_m} \left( \dot{N}_m \right)$$

showing that  $m$  is basically dependent on the rate of change of mobile dislocations during reverse flow. This could have been obtained directly from Eqs.(2) and (6) if  $\dot{v}_R$  were made equal to zero, a condition which is valid if  $N_T \gg N_m$  as assumed. If comparable, then the velocity effect must be considered. Substitution of  $m = 0$  and the kinetic equation for  $\partial N_m / \partial t_R$  previously used in Eq.(3) into Eq.(10) results in an expression applicable for logarithmic creep,

$$(11) \quad \left( \dot{N}_m \right)_{\log} = -\frac{1}{K_2 t_R^2} + \frac{\partial [(K_1 - K_3)/K_2]}{\partial t_R}$$

where  $-k_3 N_m$  has been added to the right hand side of Eq.(3) to account for stage II found in the reverse relaxation. If the reaction rate constants are considered time-independent, then at  $m = 0$ ,  $\dot{N}_m = -\frac{1}{K_2 t_R^2}$ . This also assumes a constant velocity as above, since Li<sup>(13)</sup> has shown that  $K_1 = k^1 \bar{v}$  and  $K_2 = k^1 \bar{v}$ . When  $|\dot{N}_m| < |(K_2 t_R^2)^{-1}|$ , then  $m > 0$  from the relation  $m = 1 + K_2 t_R^2 \dot{N}_m$ , the relaxation is parabolic, and the positive deviations shown in Fig. 1 result ( $t_h \cong 40$  min.). When  $|\dot{N}_m| > |(K_2 t_R^2)^{-1}|$ , then  $m < 0$ , and the negative deviations in Fig. 1 result ( $t_h < 20$  min.)

A qualitative description of A can be found by considering the following. Since A is independent of  $m$  in Eq. (6), use can be made of the expression,  $\gamma_R = A \ln t_R + C$ , for  $m = 0$ . Comparing this to Eq.(1) shows A to be  $\frac{kT}{v\theta}$ . Following a suggestion by McRickard<sup>(14)</sup> that  $v = \frac{kTn}{\tau}$ , where  $n$  is the exponent in the velocity-stress relation used in a previous discussion and  $\tau$  is the stress acting on the dislocations,

A can be approximated by  $\tau/n\theta$ . Considering this to have the characteristics of a strain, Eq. (12) can be used to represent a forward

$$(12) \quad \frac{\partial A}{\partial t_h} = \frac{L}{n\theta} \frac{\partial \tau}{\partial t_h}$$

creep equation. Assuming a generalized form of creep, then

$$\frac{\partial A}{\partial t_h} \cong \dot{\epsilon}_h \cong \frac{k''' t_h^{(m_h-1)}}{n\theta}, \quad \text{where } \frac{\partial \tau}{\partial t_h} \text{ would be equal to } \frac{k'''}{t_h^{-(m-1)}}.$$

Thus the characteristics of forward creep can be determined from reverse relaxation data by plotting  $\log \dot{A}$  vs  $\log t_h$  to obtain  $m_h$ .

Although the data shown in Fig. 7 is not sufficient to obtain accurate values of  $m_h$ , the sign can be determined directly from the A vs  $\log t_h$

curve as was done in Fig. 1 for reverse relaxation. Ferrovac "E"

shows a large positive deviation and 700ppm C-iron a smaller positive

deviation. This parabolic behavior is typical of forward creep

processes; for example, Andrade's <sup>(15)</sup>  $\beta$  creep equation  $\dot{\epsilon} = \epsilon t^{-2/3}$ ,

where  $m = +\frac{1}{3}$ .

In irradiated "E", A appears to be logarithmic for the first minute, then decreases with time. This decrease in A can be a result of either a decreasing driving force for reverse flow,  $\frac{\partial \tau}{\partial t_h}$  negative, or a decrease in  $N_m$ , the number of mobile dislocations. In the decarburized iron,  $\frac{\partial \tau}{\partial t_h}$  appears to be zero and no net change in the number of dislocations contributing to reverse flow is observed.

### Model

A model for forward and reverse relaxation can be offered on the basis of change in dislocation configuration and the relative ease of dislocation movement. The steps in the forward process, as suggested

by Garofalo<sup>(16)</sup> for example, are movement of dislocations in the lattice, formation of tangled networks, redistribution of dislocations in the tangle, and time dependent pinning of the dislocations. In the reverse process the steps are inhibition of dislocation movement by tangling (stage I), pinning by a carbon atmosphere (stage II), and possible increase in  $N_m$  by unpinning of the dislocations pinned during the forward process (stage I<sup>1</sup>).

That stage II and the decrease in A at  $t_h > 40$  min. in Ferrovac "E" are caused by pinning can be shown by yield point analysis; that is, measurement of the appearance or disappearance of a yield point under varying load and unload cycles. This was done for the Ferrovac "E", with representative results shown in Fig. 8. After a holding time of 120 min., a reloaded sample showed the appearance of a pronounced upper yield point. At shorter times the yield point diminished and at times less than 30 min. was not observed on reloading. When the load was completely removed, and then the specimen reloaded, a yield point was found only after high relaxation times, including the  $t_h = 40$  min. sample. After a holding time of 120 min., a specimen was unloaded and reloaded after 30 sec. of reverse relaxation showing the appearance of a yield point. From this series, it can be postulated that the decrease in A after a holding time of 40 min. is produced by pinning of mobile dislocations and a low initial reverse relaxation rate. Upon load release, the high unbalanced internal stress field causes unpinning, thus adding dislocations to the relaxation process and resulting in the positive deviation ( $m > 0$ ) of Fig. 2. In the  $t_h = 120$  min. sample, unpinning did not occur immediately and a yield point was observed on reloading. Reloading after a large

relaxation time showed the occurrence of pinning during relaxation, and was related to the inhibition of dislocation motion by accumulation of an atmosphere during stage II.

The dislocation configuration characteristic of 10% strain consists mostly of tangled networks, as shown by Keh and Weissmann<sup>(1)</sup>. The size and density of the networks depends upon the strain rate and, as indicated by Michalak<sup>(5)</sup>, the faster the rate the less time that is available for dynamic recovery by cross glide and the lower the tangle density. In the present work, a comparatively high rate was used ( $0.157 \text{ min.}^{-1}$ ) to achieve a non-equilibrium dislocation structure prior to the forward relaxation cycle. During the holding period, where the strain rate is much lower, "free" dislocations will migrate to the tangle regions and the dislocations within the tangles will reorient to a more stable configuration, the relative rates depending on the ease of movement through the lattice and cross glide. This redistribution is manifested mainly as a change in the A parameter. In Ferrovac "E", there is an increase in A indicating that the "free" dislocations move into the high stress tangle regions raising  $N_m$  and the driving force  $\tau$ , simultaneously, resulting in a higher relaxation rate. The observation that A increases up to a comparatively long holding time of 40 min. indicated that rearrangement of the dislocations within the tangle was a major contributor to raising  $\tau$  and perhaps  $N_m$  by double cross glide within the tangle.

The decrease in A after 40 min. is a result of a decrease in  $N_m$  by pinning as previously shown. This can occur by either diffusion of carbon atoms to the tangle sites (strain aging) or by increased

tangling and immobilization by the cross gliding segments. The results of the 700 ppm C-iron samples are of interest on this point. It would be expected that formation of a carbon atmosphere would occur at least as rapidly as in the Ferrovac "E", but it was found that a decrease in A and reverse unpinning did not appear until after a much longer holding time. The observations that the absolute magnitude of A at the onset of forward pinning is about the same in both materials and that  $m_h$  is less positive in the high carbon iron (low Å) indicates that both the stress concentration within the tangle and the ability to cross glide have an influence on the pinning characteristics. Apparently, carbon acts to restrict cross glide resulting in the slow immigration of dislocations to the tangle and redistribution of dislocations within the tangle. It must then take longer to build up the driving force for redistribution of the tangled dislocations and subsequent pinning. The function of the carbon in the tangle would appear to be the restriction of the cross glide necessary for dislocation-dislocation pinning as well as atmosphere pinning. It is not certain at this time that carbon pinning is not influencing the data; the possibility exists that the dislocations are already saturated at low  $t_h$  in the high C material and therefore no discontinuity in A would be observed. The onset of reverse unpinning (stage I<sup>1</sup>) could merely be dependent on the buildup of a large enough driving force. One experimental finding that suggests the occurrence of carbon pinning is the onset of stage I<sup>1</sup> at about the same holding time at which the value of m in stage II decreases.

The observation that  $\dot{A}$  does not become negative in the decarburized samples does not necessarily indicate that carbon is necessary for pinning. Since cross glide is extremely easy in this material, no "free" dislocations exist after the loading cycle and the dislocations are already present in the highly tangled state that other materials approach only after a prolonged holding period. This is also indicated by the insensitivity of  $\dot{A}$  to holding time. The uniformly low value of  $A$  attests to the limited number of mobile dislocations; also, the low value of  $m$  in stage I shows the relative ease of tangling.

#### Irradiation Effects

The effects of irradiation on the forward and reverse processes suggest several important aspects of the damage. The high value of  $A$  obtained prior to the holding period indicates that the number of "free" dislocations able to contribute to reverse relaxation is initially high. Such would be the case if the dislocation networks were confined to more localized areas than in the homogeneous arrays usually found, and that these networks were in a comparatively untangled state so that both the driving force for reverse flow and  $N_m$  are large. This would be similar in effect to the configurations in certain FCC and HCP metals where dislocation pile-up is common and reverse movement easy. To accomplish this, the irradiation damage must restrict slip to a lower number of slip systems and reduce cross glide. The decreased tendency for tangling is indicated by the approach of stage I to a logarithmic relaxation. This type of behavior is supplemented by observations of Chow<sup>(17)</sup> that slip

lines on the surface of irradiated "E" are straighter, more pronounced, and more widely spaced than those in unirradiated "E". The logarithmic increase in A at holding times  $< 1$  min. also indicates a similarity to the "pile-up" behavior, although subsequent interactions in the high stress regions quickly reverse the trend. The second effect of the damage appears to be the removal of carbon from the lattice, probably by carbon-defect pairs, as proposed by Fujita and Damask<sup>(18)</sup>. This is indicated by the absence of stage II pinning after a 1 min. holding time. The high negative values of m obtained initially in stage II must be a result of movement of the "free" dislocations over comparatively large distances through the damage and deformation "debris." After the 1 min. delay, the dislocations had moved into the local configuration and only short range motion occurred during reverse strain. It is also possible that the "debris" becomes absorbed by the irradiation defects. The absence of forward pinning could be attributed to either inhibition of cross glide or by removal of the carbon.

Work is presently in progress concerning the effects of temperature on the forward and reverse mechanisms proposed in the preceding discussion. Although only a small amount of data is available, it is becoming apparent that the reverse relaxation is moving towards parabolic behavior at lower test temperatures, showing a decreased tendency for tangling or cross glide.



## SUMMARY

Combination forward relaxation-reverse relaxation tests have been run on samples of Ferrovac "E" iron, irradiated Ferrovac "E", decarburized iron, and iron-700ppm C at 300°K and 0.10 strain. The findings are as follows:

- 1) The reverse relaxation data were plotted according to the general creep equation,  $\dot{\gamma}_R = A t_R^{(m-1)}$ . Two stages were noted, stage I  $< 1$  min. and stage II  $> 2$  min. Both provided a negative value for  $m$  indicating a high rate of removal of mobile dislocations.
- 2) Stage I was associated with reverse tangling of dislocations. The results of Ferrovac "E", decarburized iron, and 700ppm C-iron fell within a small range of  $m(-.2 > m > -.36)$ , although decarburization produced the lowest values,  $-.36$ , indicating an increase in tangling tendency. Irradiation resulted in an approach to logarithmic behavior ( $m = 0$ ) and inhibition of cross glide and tangling.
- 3) Stage II was associated with pinning by a carbon atmosphere. Decarburization resulted in logarithmic behavior during this cycle of relaxation and 700ppm C caused lower  $m$  (more negative) than found in Ferrovac "E". Irradiation again resulted in logarithmic behavior indicating removal of carbon from the lattice by formation of carbon-defect pairs.
- 4) Forward relaxation involved movement of "free" dislocations into tangled networks and redistribution of the dislocations in tangle. Pinning of the dislocations in tangle reduced  $A$  and occurred

by dislocation-dislocation and carbon atmosphere (strain aging) interactions. Unpinning took place during the reverse cycle (stage I<sup>1</sup>). The presence of pinning produced during forward and reverse relaxation was detected by yield point analysis.

5) The effect of carbon addition on forward relaxation seemed to be inhibition of cross glide rather than atmosphere pinning.

6) The dislocation configuration produced during the loading cycle in irradiated iron appeared to have a higher number of mobile dislocations and a lower degree of tangling than in unirradiated iron. As mentioned in (2) this reflects restricted cross glide and operation of a limited number of slip systems.

This testing technique shows great promise for separate study of the various contributors to forward relaxation and for movement of dislocations through the lattice under controlled testing conditions and structural changes.

### ACKNOWLEDGMENTS

The author wishes to thank J.G. Y. Chow and S.B. McRickard of the Brookhaven National Laboratories for many stimulating discussions, and the National Science Foundation for partial support under NSF Grant GP-3062. This work was also sponsored in part by the U. S. Atomic Energy Commission through the Brookhaven National Laboratories.

## BIBLIOGRAPHY

1. A.S. Keh and S. Weissmann, Electron Microscopy and Strength of Materials, Interscience Pub., N.Y., p 231(1963).
2. H. Conrad, J. Metals, 16, 582(1964).
3. W.G. Johnston and J.J. Gilman, J. Appl. Phys., 30, 129(1959).
4. D.F. Stein and J.R. Low, Jr., *ibid*, 31, 362(1960).
5. J.T. Michalak, Acta Met., 13, 213(1965).
6. F.W. Noble and D. Hull, Acta Met., 12, 1089(1964).
7. C.S. Barrett, J. Metals, 197, 1652(1953).
8. B.I. Edelson and W.D. Robertson, Acta Met., 2, 583(1954).
9. J.M. Roberts and N. Brown, Acta Met., 11, 7(1963).
10. J.C.M. Li, Acta Met., 11, 1269(1963).
11. C. Crussard, Trans. ASM, 57, 778(1964).
12. D.F. Stein, J.R. Low, Jr., and A.U. Seybolt, Acta Met., 11, 1253(1963).
13. J.C.M. Li, Acta Met., 13, 37(1965).
14. S.B. McRickard, private communication.
15. E.N. da C. Andrade, P.R.S., A. 84, 1(1910).
16. F. Garofalo, Fundamentals of Creep and Creep-Rupture in Metals, Macmillan, N.Y., pp 123-3(1965).
17. J.G.Y. Chow, private communication.
18. F.E. Fujita and A.C. Damask, Acta Met., 12, 2(1964).

## Figure Captions

- Figure 1 - Reverse relaxation data for Ferrovac "E" showing deviations from logarithmic behavior. The "initial" slope increases for holding times up to 20 minutes then decreases. The decrease in slope coincides with a changeover from negative to positive deviation although the final stage in all relaxation curves is a negative deviation.
- Figure 2 - The data of Fig. 1 replotted as  $\log \dot{\gamma}_R$  vs  $(m-1) \log t_R$ . Two stages of relaxation are noted for holding times up to 20 min.: stage I  $< 1$  min., stage II  $> 2$  min. The curves are approximately parallel in the two stages, the relative displacement being dependent on the parameter A in  $\dot{\gamma}_R = At_R^{(m-1)}$ . The values of m in the two regions are negative showing the deviation inferred in Fig.1. For holding times  $\geq 40$  min., m becomes positive in the first stage (stage I<sup>1</sup>), then the curves become parallel to stage II of the lower holding time curves. All three stages are present in the  $t_h = 120$  min. curve.
- Figure 3 - Effects of decarburization on the characteristic reverse relaxation curve. In stage I m is slightly lower than that of the Ferrovac "E", and stage II becomes logarithmic showing the dependence of the latter stage on carbon. A is independent of holding time.
- Figure 4 - Effects of excess carbon. Stages I and II are similar to those of the Ferrovac "E", except that the onset of stage II is delayed. The positive deviation ( $m > 0$ ) occurs after a much longer holding time.
- Figure 5 - Irradiation of Ferrovac "E" produces logarithmic behavior in both stages I and II. There is a large initial ( $t_h < 1$  min) negative deviation in stage II which quickly disappears.
- Figure 6 - Summary curves for values of m. Ferrovac "E", decarburized iron, and 700ppm C-iron have approximately the same values of m in stage I, the decarburized samples being lowest. The onset of positive m occurs much sooner in Ferrovac "E" than in the 700ppm C material, and no positive deviation is noted for either decarburized or irradiated samples. The values of m for stage II are lower than those of stage I except for the decarburized samples in which m approaches zero in the second stage. The lowest values of m were obtained in the irradiated and annealed samples.

Figure 7 - Summary curves for values of A. Ferrovac "E" and 700ppm C-iron deviate positively from the relation,  $A = clnt_h$ , the former showing the largest deviation. The results of the decarburized samples are independent of holding time, and the absolute magnitude of A is low. In the Ferrovac "E" samples, A decreases at holding times  $> 40$  min. The magnitude of A in the irradiated samples is highest, but comparatively independent of holding time; at times  $< 1$  min. A increases logarithmically, then decreases slightly after 1 min.

Figure 8 - Yield point analysis of Ferrovac "E". (a) Reloading after a holding time of 120 min. produced a yield point, but none appeared after the short time of 20 sec. (b) After releasing the load, a yield point was found after a reverse relaxation of 50 min. (c) A yield point was found after a reverse relaxation of 30 sec. in the  $t_h = 120$  min. sample. Subsequent unloading and reloading produced a yield point only after a prolonged reverse relaxation time.

FERROVAC "E"

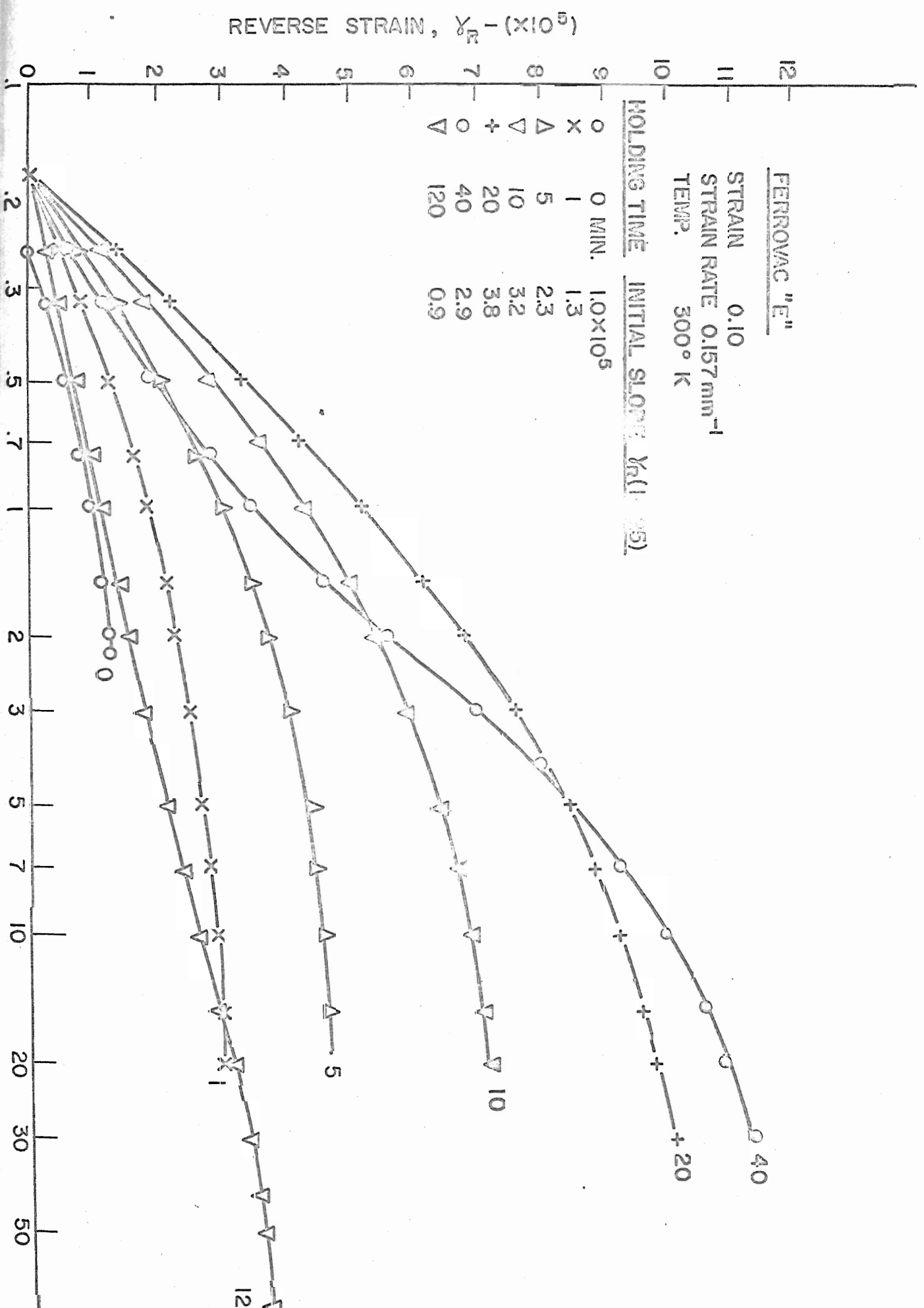
STRAIN 0.10

STRAIN RATE 0.157 mm<sup>-1</sup>

TEMP. 300° K

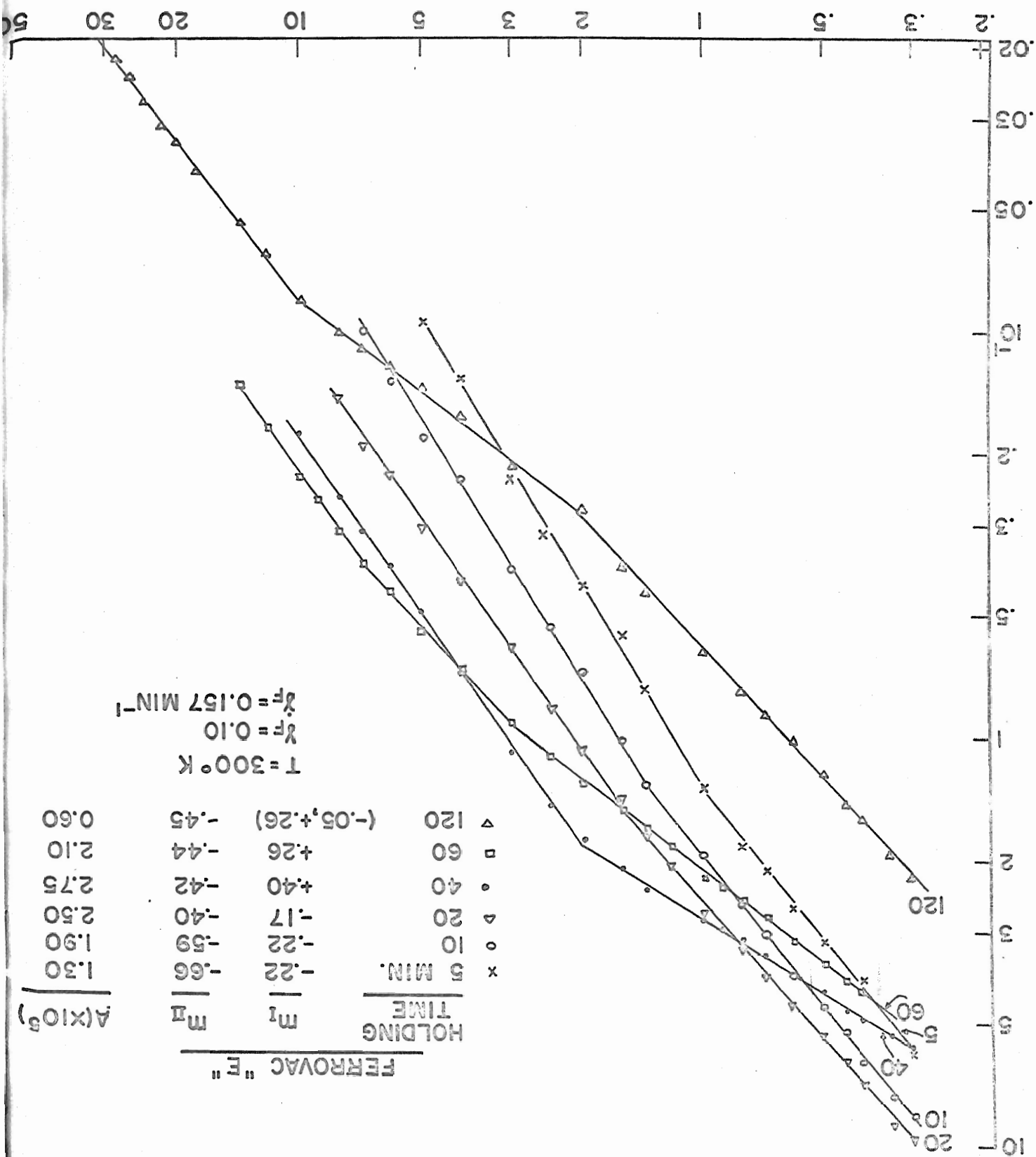
HOLDING TIME INITIAL SLOPE  $\gamma_R$  (1.95)

HOLDING TIME	INITIAL SLOPE $\gamma_R$ (1.95)
0 MIN.	1.0x10 <sup>5</sup>
1	1.3
5	2.3
10	3.2
20	3.8
40	2.9
120	0.9



REVERSE STRAIN RATE,  $\dot{\gamma}_R - \text{MIN}^{-1} (\times 10^5)$

REVERSE RELAXATION TIME - MINUTES



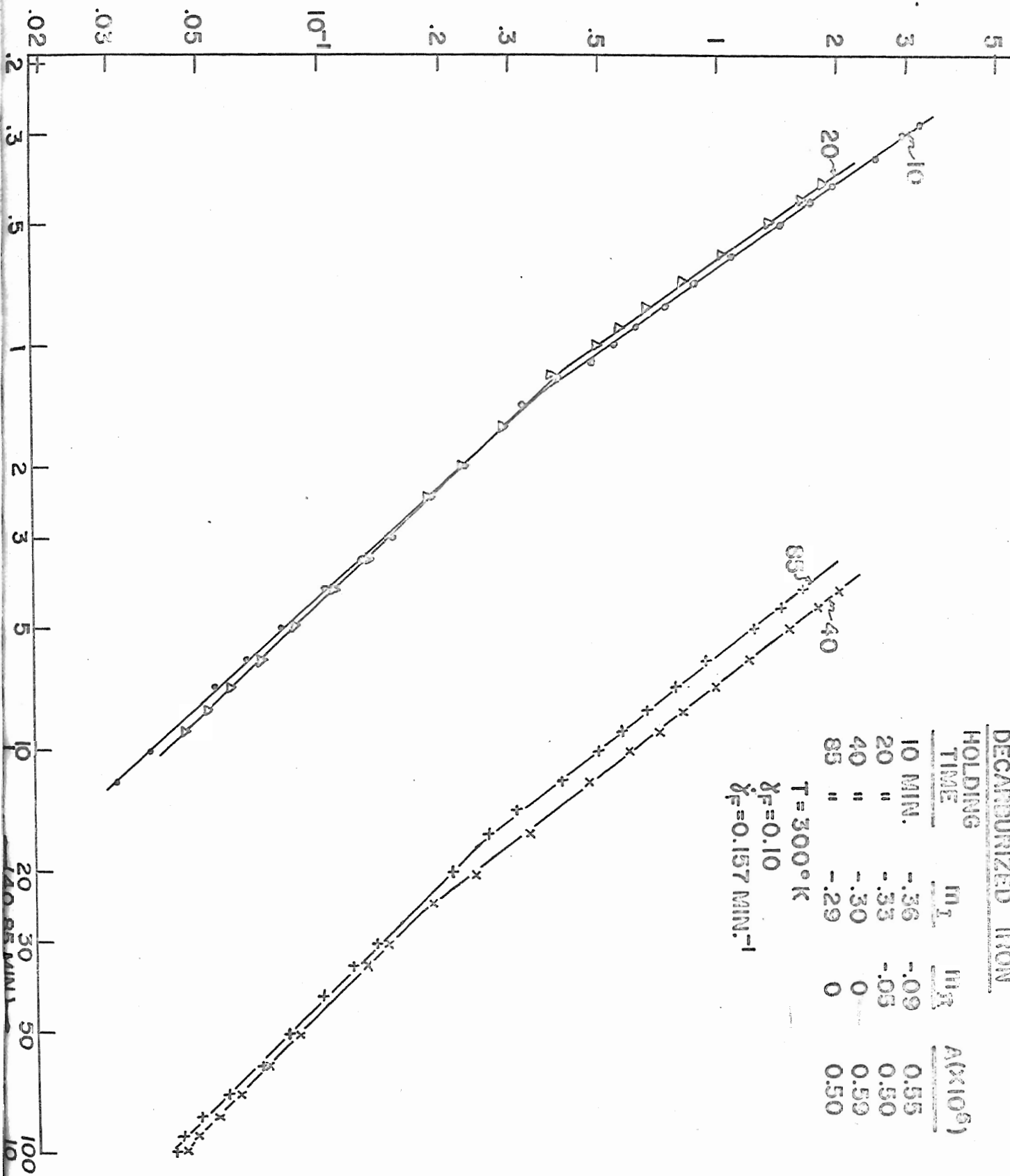
$T = 300^\circ \text{K}$   
 $\dot{\gamma}_F = 0.10$   
 $\dot{\gamma}_F = 0.157 \text{ MIN}^{-1}$

HOLDING TIME	$M_I$	$M_{II}$	$A (\times 10^5)$
120	(-0.05, +.26)	-0.45	0.60
60	+0.26	-0.44	2.10
40	+0.40	-0.42	2.75
20	-0.17	-0.40	2.50
10	-0.22	-0.59	1.90
5 MIN.	-0.22	-0.66	1.30

FERROVAC "E"



REVERSE STRAIN RATE,  $\dot{\gamma}_R - \text{MIN.}^{-1} (\times 10^5)$



DECARBURIZED IRON

HOLDING TIME	$\ln T$	$\ln \dot{\gamma}_R$	$A (\times 10^5)$
10 MIN.	-.36	-.09	0.55
20 "	-.33	-.05	0.50
40 "	-.30	0	0.59
85 "	-.29	0	0.50

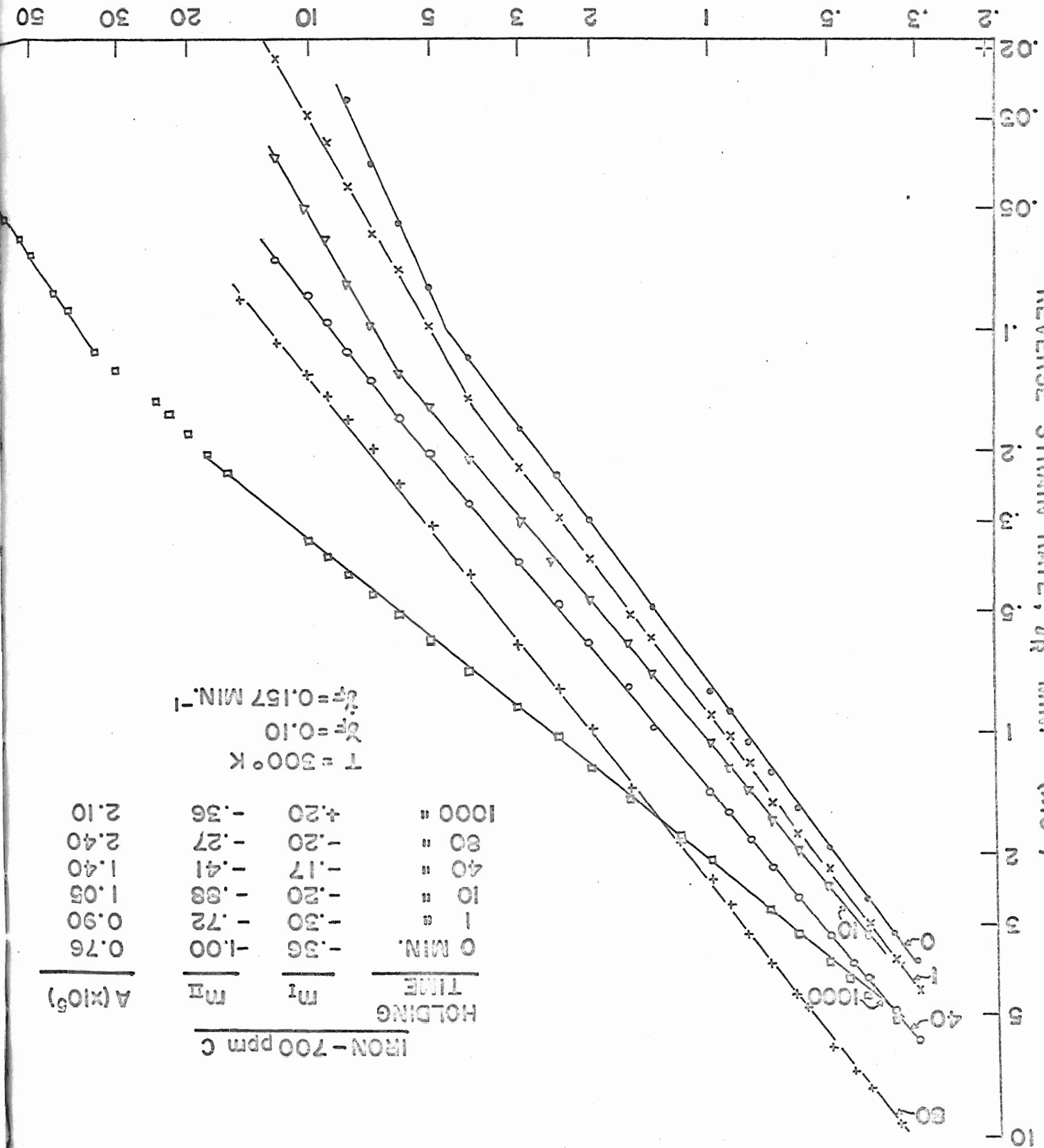
85  
40

$T = 300^\circ \text{K}$   
 $\dot{\gamma}_F = 0.10$   
 $\dot{\gamma}_F = 0.157 \text{ MIN.}^{-1}$

20 30 50 100  
 100 85 MIN.

REVERSE RELAXATION TIME - MINUTES

REVERSE STRAIN RATE,  $\dot{\epsilon}_R$  - MIN.<sup>-1</sup> - (X10<sup>5</sup>)



T = 300°K  
 $\dot{\epsilon}_R = 0.10$   
 $\dot{\epsilon}_R = 0.157$  MIN.<sup>-1</sup>

HOLDING TIME		A (X10 <sup>5</sup> )	
MIN.	m <sub>I</sub>	m <sub>II</sub>	
0	-.36	-1.00	0.76
1	-.30	-.72	0.90
10	-.20	-.88	1.05
40	-.17	-.41	1.40
80	-.20	-.27	2.40
1000	+.20	-.36	2.10

IRON-700 ppm C



